International Core Journal of Engineering Volume 12 Issue 3, 2026
ISSN: 2414-1895 DOI: 10.6919/ICJE.202603_12(3).0026

Effect of TiO_2 Nanoparticles on Wetting and Friction Wear Properties of Bionic Textured UHMWPE for Nepenthes

Xuyang Nie[1], Wen Zhong[1,*], Jun Tang[1], Siqiang Chen[2]

[1] School of Mechanical Engineering, Xihua University, Chengdu, Sichuan 610031, China

[2] Luzhou Vocational School, Luzhou, Sichuan, China

[*]Corresponding author: Wen Zhong (Email: zw1019@126.com)

Abstract

To address material adhesion and wear issues of equipment in the food and pharmaceutical fields, pitcher plant's crescent-shaped inner wall structure was used as the bionic prototype. Textured UHMWPE/TiO_2 composites with TiO_2 mass fractions of 0–20wt% were prepared via solution blending-molding-ultraviolet laser texturing. The regulation mechanism of TiO_2 content on the material's wettability and tribological properties was investigated. The results show that the blank textured UHMWPE exhibits a water contact angle of 132.5° and a friction coefficient as low as 0.13. After introducing TiO_2, the water contact angle fluctuates in a "decrease-rise-fall" trend, and the hydrophobicity is weakened overall. The friction coefficient increases with the rise of TiO_2 content; the 20wt% group shows a 346.2% increase compared with the blank textured group, and the high-content groups (15–20wt%) present severe fluctuations in friction curves. The wear loss increases significantly with increasing TiO_2 content, and the wear mechanism gradually shifts from adhesive wear to abrasive wear-dominated. This study provides key references for the component optimization of bionic UHMWPE composites.

Keywords

Pitcher Plant-bionic Texture; TiO_2/UHMWPE Composite; Wettability; Tribological Property.

1. Introduction

In industrial sectors such as food, pharmaceuticals, and chemicals, material adhesion to equipment surfaces often leads to reduced production efficiency, product contamination, and equipment wear [1-2]. Ultra-high molecular weight polyethylene (UHMWPE), with its excellent corrosion resistance, impact toughness, and biocompatibility, has become an ideal material for manufacturing critical components [3-5]. However, the hydrophobicity and wear resistance of single UHMWPE still need improvement under harsh operating conditions [6-7]. Surface biomimetic texturing and nanoparticle composites are effective strategies for optimizing polymer surface properties. The micro-nano hierarchical structure of Nepenthes niger surfaces demonstrates potential for hydrophobicity and anti-friction/wear performance through air cushion effects [8-9]. Nanometer-sized titanium dioxide (TiO_2), due to its high stability and hardness, is commonly used to enhance the mechanical and tribological properties of polymers [10-11]. For instance, the unique hydrophobicity of Nepenthes niger insect-trapping traps provides valuable insights for research [12], while their micro-nano structures hold promise for applications in microfluidic detection, microfluidics, self-cleaning, and chip cooling [13]. Additionally, laser-etched biomimetic superlubricant surfaces of Nepenthes niger showcase superhydrophobic and superlubricant properties achieved through specific processing techniques [14-

ISSN: 2414-1895 DOI: 10.6919/ICJE.202603_12(3).0026

15]. However, existing studies predominantly focus on synergistic effects while neglecting the disruption of textural integrity caused by nanoparticle aggregation. Particularly in Nepenthes niger biomimetic systems, the regulatory mechanisms and intrinsic principles governing the influence of TiO_2 nanoparticle content on UHMWPE wettability and tribological performance remain unclear, leaving relevant systematic research in this area unexplored. Based on this, this study prepared bionic-textured UHMWPE composites with varying TiO_2 content in Nepenthes, and investigated the effects of TiO_2 content on the wettability and friction-wear properties of the materials. The compatibility of the system was clarified, providing experimental evidence for the optimization of composite components and process design, thereby promoting its industrial application.

2. Experimental Section

2.1 Raw and Processed Material

UHMWPE (Dongguan Wangda Plastic Raw Materials Co., Ltd., molecular weight 5×10^7) and TiO_2 (Bisley New Materials Suzhou Co., Ltd., rutile type, purity 99.9%)

2.2 Equipment and Instruments

Ultraviolet laser marking machine (Model TD-3500, Dandong Tongda Technology Co., Ltd.); Electronic balance (precision 0.0001g); Constant temperature magnetic stirrer; Vacuum drying oven; Dynamic contact angle tester (Model SDC-350, Dongguan Shengding Precision Instrument Co., Ltd.); Reciprocating friction and wear tester (Model MWF-02, Sichuan Jiaoyang Technology Co., Ltd.); Mini flat plate vulcanization tester (Model ST-15YP, Kunshan Lugong Precision Instrument Co., Ltd.); Spectral confocal 3D contour measuring instrument (Model SM-5000, Sixian Optoelectronic Technology Shanghai Co., Ltd.); Super depth-of-field microscope (Model RS-V1, Huandian Technology Shanghai Co., Ltd.); Agate mortar.

2.3 Sample preparation

This study utilized the crescent-shaped structure of the inner wall of the natural pitcher plant as a biomimetic prototype. First, a composite powder was prepared using the solution blending method. Ultra-high molecular weight polyethylene (UHMWPE) and titanium dioxide (TiO_2) nanoparticles were precisely weighed in predetermined proportions and added to a beaker containing 100 mL of anhydrous ethanol. The mixture was then heated and stirred on a constant-temperature magnetic stirrer at 500 rpm and 60±2°C until the anhydrous ethanol completely evaporated. Subsequently, the mixture was dried in an 80°C vacuum drying oven for 6 hours. After manual grinding to remove any clumps, the material was dried again in an 80°C vacuum drying oven for 1 hour. The resulting homogeneous composite powder was stored in a moisture-proof cabinet for later use. Next, 2.2±0.005 g of the composite powder was precisely weighed and evenly poured into a specialized mold. The mold was preformed under 5 MPa pressure for 10 minutes. The preformed mold was then placed in a small flat vulcanization apparatus, where it was heated to 200°C and hot-pressed under 5 MPa pressure for 30 minutes. After hot-pressing, the mold was naturally cooled for 30 minutes to room temperature for demolding. The edges of the samples were trimmed to remove burrs, yielding smooth flat substrates with a diameter of Φ30 mm and a thickness of 3 mm. Finally, a UV laser marking machine was used to process the surface of the flat substrates with pitcher plant biomimetic textures, setting the texture spacing at 200 μm in the transverse direction and 100 μm in the longitudinal direction. By adjusting the TiO_2 addition ratio during the raw material blending stage, a series of textured UHMWPE/TiO_2 composite materials with TiO_2 mass fractions of 0 wt%, 5 wt%, 10 wt%, 15 wt%, and 20 wt% were prepared, as shown in Figure 1.

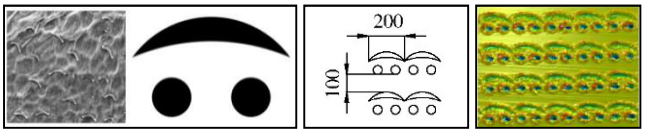

Figure 1. Bionic Texture of Nepenthes

ISSN: 2414-1895 DOI: 10.6919/ICJE.202603_12(3).0026

2.4 Testing and Characterization

2.4.1 Wettability Test

Clean the sample surface with anhydrous ethanol. After drying, place the sample on the stage of a dynamic contact angle measurement instrument and adjust the lens position relative to the stage. Add ultrapure water to the sample surface using a micropipette. Immediately photograph the sample upon droplet contact, then calculate the contact angle through software fitting. Perform five measurements at different positions on the same sample surface. After removing the highest and lowest values, calculate the average.

2.4.2 Wear And Tear Test

A 6mm-diameter 304 stainless steel ball with surface roughness (Rmax=0.02μm) was used as the friction pair in a dry friction test conducted on a reciprocating friction wear tester. The test parameters were set as follows: 20N test force, 8mm reciprocating stroke, 2Hz reciprocating frequency, 1800s test duration, 1N/s load rate, and temperature maintained at 25±2℃. Each test was repeated three times, with automatic data acquisition of friction coefficient, test load, and time.

2.4.3 Wear Morphology and Wear Scale Characterization

The wear morphology of the samples was measured by a spectral confocal 3D contour measuring instrument, and the wear rate was calculated by the built-in software. The surface morphology of the samples before and after the test was observed by a super-depth microscope, and the wear characteristics were analyzed.

3. Results and Analysis

3.1 Effect of TiO_2 Nanoparticles on Wetting Properties of Nepenthes Tessile

As shown in Figure 2, the water contact angle of a single Nepenthes-like UHMWPE sample (0% TiO_2) was 132.5°, exhibiting stable Cassie-Baxter state hydrophobicity [16]. This results from the micro-nano-textured structure mimicking Nepenthes reducing the actual liquid-solid contact area and inhibiting liquid spreading. After introducing TiO_2, the composite sample's water contact angle showed a fluctuating trend of "decreased-rise-decreased": the 5wt% group decreased to 102.7°, the 10wt% group recovered to 105.8°, the 15wt% group increased to 118.2°, and the 20wt% group decreased to 112.1°. This pattern aligns with TiO_2' s surface hydrophilic-hydrophobic modulation characteristics, demonstrating the synergistic effect of hydrophilic TiO_2 and the textured surface. Low TiO_2 content (5wt%) directly weakened the hydrophobicity, causing a sharp drop in contact angle; moderate content (10wt%, 15wt%) ensured uniform particle dispersion without compromising texture integrity, mitigating negative effects; high content (20wt%) led to TiO_2 agglomeration disrupting the texture, weakening the hydrophobic effect, ultimately resulting in a trend of reduced hydrophobicity and enhanced hydrophilicity.

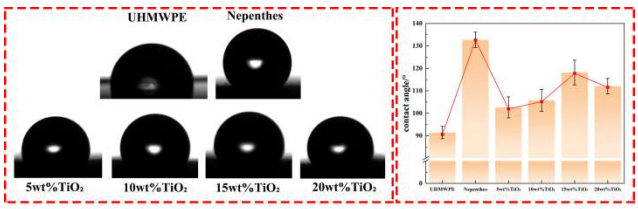

Figure 2. Wetting properties of different samples

3.2 Effect of TiO_2 Nanoparticles on Friction Coefficient of Nepenthes texans

As shown in Figure 3, the friction coefficient of UHMWPE was 0.16. The tribological performance of the blank pitcher plant-textured UHMWPE sample was significantly optimized, with an average friction coefficient of only 0.13 and a stable friction curve. This was attributed to the texture grooves storing air, reducing the contact area between friction pairs, and suppressing adhesive friction. After

ISSN: 2414-1895 DOI: 10.6919/ICJE.202603_12(3).0026

TiO_2 doping, the composite samples exhibited higher friction coefficients than the blank group, with an increasing trend as TiO_2 content increased: the 5wt% group had a friction coefficient of 0.12, while the 10wt%, 15wt%, and 20wt% groups progressively increased to 0.43,0.61, and 0.58, respectively. Compared to the blank pitcher plant texture, the 20wt% group showed a 346.2% increase. It should be noted that TiO_2 can reduce friction by filling surface voids in some composites, but this effect was not observed in this system [17]. The high-content groups (15wt%, 20wt%) exhibited severe fluctuations in the friction curve, frequent spikes, and significantly reduced stability, indicating the presence of irregular abrasive particles during wear. The core mechanism lies in insufficient dispersion of TiO_2 in the matrix, leading to agglomeration that disrupts the integrity of the texture grooves. This results in the loss of air-storing anti-friction effects, increased contact area, and the formation of hard abrasive particles due to the detachment of agglomerated particles, ultimately causing abrasive wear and leading to increased friction coefficients and reduced stability.

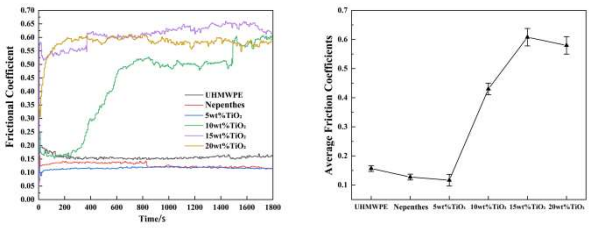

a-Friction coefficients of different samples b-Average friction coefficients of different samples

Figure 3. Tribological properties of different samples

3.3 Effect of TiO_2 Nanoparticles Content on Textural Wear and Wear Morphology of Nepenthes

3.3.1 Variation Law of Wear

As illustrated in Figure 4, the effect of TiO_2 content on sample wear exhibits a distinct gradient: The 5wt% TiO_2 group shows the least wear (Figure b), with correspondingly shallow three-dimensional wear patterns (Figure a). When TiO_2 content increases to 20wt%, wear significantly intensifies, and the wear zones in high-content groups reveal no visible texture structure, indicating severe material degradation. This phenomenon stems from TiO_2 nanoparticles 'hardening effect, which increases surface texture vulnerability to stress concentration. At low concentrations, the stress concentration effect remains minimal, limiting wear resistance. However, high concentrations exacerbate TiO_2 agglomeration, amplifying stress concentration's detrimental effects while compromising texture integrity, ultimately causing substantial wear reduction. The combination of weak stress concentration and intensified agglomeration at high concentrations further diminishes the material's wear resistance.

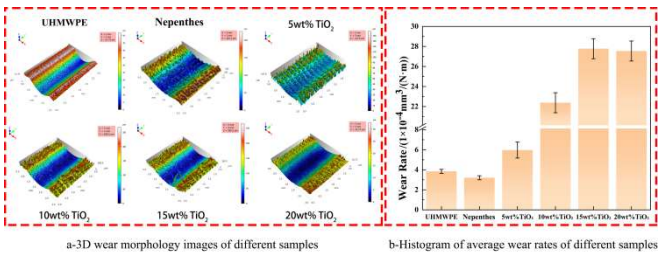

a-3D wear morphology images of different samples b-Histogram of average wear rates of different samples

Figure 4. Wear performance of different samples

3.3.2 Wear Morphology Characteristics

As shown in Figure 5, the wear morphologies of different samples exhibited significant variations: The original UHMWPE surface displayed only uniform shallow scratches, corresponding to adhesive wear; the blank pitcher plant texture group retained partial texture structures with only localized minor plastic deformation; the 5wt% TiO_2 group retained residual textures, presenting mild plastic

ISSN: 2414-1895 DOI: 10.6919/ICJE.202603_12(3).0026

deformation protrusions; the 10wt% TiO_2 group exhibited completely disappeared textures, with surface features of corrugated plastic flow accompanied by shallow plow furrows, indicating wear combining adhesive wear with minor abrasive wear; the 15wt% TiO_2 group displayed dense plow furrows and spalling pits, with abrasive wear being predominant; the 20wt% TiO_2 group was covered by deep plow furrows and large concave pits, exhibiting the most pronounced abrasive wear characteristics. With increasing TiO_2 content, the wear mechanism progressively shifted from adhesive wear to abrasive wear dominance, a change highly consistent with the deterioration pattern of friction performance.

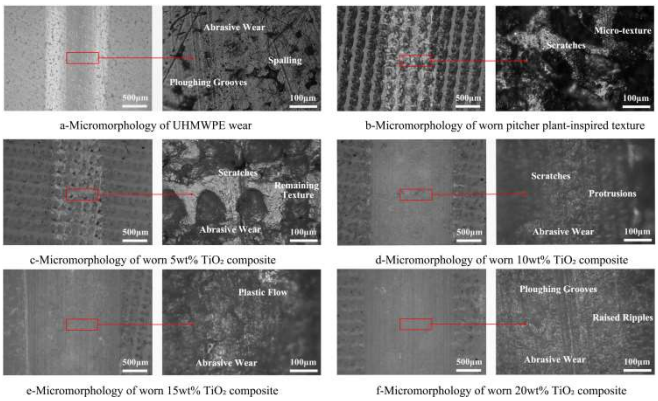

Figure 5. Microscopic wear morphology of different samples

4. Conclusion

(1) The biomimetic texture of Nepenthes can significantly improve the hydrophobicity and tribological properties of UHMWPE: the water contact angle of the blank texture group reached 132.5° (stable Cassie-Baxter state hydrophobicity), and the friction coefficient decreased to 0.13. This advantage stems from the texture's ability to reduce the liquid-solid/friction pair contact area.

(2) The wettability of textured UHMWPE is modulated by TiO_2 content: the contact angle exhibits a "decrease-increase-decrease" trend with increasing TiO_2 content. Low TiO_2 content weakens hydrophobicity, moderate content mitigates degradation due to uniform particle dispersion, while high content disrupts texture through agglomeration. Overall, the system demonstrates weakened hydrophobicity and enhanced hydrophilicity.

(3) The friction coefficient of the composite samples increased with the increase of TiO2 content, and the increase of the friction coefficient of the composite samples was 346.2% compared with the blank texture group.

(4) The increase in TiO_2 content exacerbates wear: the 5wt% group exhibits the least wear, while the 20wt% group shows a significant increase in wear with complete loss of texture. As TiO_2 content rises, the wear mechanism gradually shifts from adhesive wear to abrasive wear dominance, consistent with the deterioration of friction performance. The primary cause is that high TiO_2 content aggregates to amplify stress concentration and disrupt texture integrity.

Acknowledgments

The authors declare that there are no additional acknowledgments to be made for this work.

References

[1] YAO Guangyuan, LIU Yuqiang, LIU Jingcai, XU Ya. Research on the generation properties and pollution control of pharmaceutical manufacturing industry in China[J]. Journal of Environmental Engineering Technology, 2021, 11(6): 1258-1265.

[2] All visible pores. Common causes of corrosion and anti-corrosion strategies for petrochemical equipment [J]. Engineering Construction, 2023,6(12):67-69.

ISSN: 2414-1895 DOI: 10.6919/ICJE.202603_12(3).0026

[3] Ye Zhuoran, Luo Liang, Pan Haiyan, et al. Research Status and Analysis of Ultra-High Molecular Weight Polyethylene Fibers and Their Composites [J]. Acta Materiae Compositae Sinica, 2022,39(9).

[4] Huang Anping, Zhu Bochao, Jia Junji, et al. Development and Application of Ultra-High Molecular Weight Polyethylene [J]. Polymer Bulletin, 2022,25(4):127-132.

[5] Feng Yuan, Wang Hongqiu, Yu Junrong. Research progress on wear mechanism and wear-resistant modification of ultra-high molecular weight polyethylene [J]. Polymer Bulletin, 2022,35(10):54-62.

[6] Zhao Yamei, Huo Mengdan, Cao Tingting, et al. Research progress on improving the mechanical durability of superhydrophobic materials [J]. Acta Materiae Compositae Sinica, 2023,40(4).

[7] Sun Juntao. Design and Research Progress of High-Intensity Superhydrophobic Surfaces [J]. Material Sciences, 2024,14:319.

[8] Mao Yukun, Chen Wengang. Surface texturing technology improves tribological performance of engine crankshaft bearings [J]. Science Technology & Engineering, 2022,22(34).

[9] Li Yunkai, Wang Youqiang, Kan Guangxiao, et al. Finite element analysis of tribological properties of water-lubricated bearings mimicking the structure of Nepenthes niger[J]. Journal of Tribology, 2021,41(3):344-356.

[10] Zhou Maomao, Jiang Yang, Xie Yuhui, et al. Preparation, modification and application of nano-titanium dioxide in polymer-based composites [J]. Acta Materiae Compositae Sinica, 2022,39(5).

[11] Zhang Ruizhu, Zhang Guoyu, Wei Changtao, et al. Research on Wear Resistance Enhancement of Epoxy Resin by Nano-Titanium Dioxide/Glass Flake Co-Enhancement [J]. Electroplating & Finishing, 2024,43(3).

[12] Wang Lixin, Wu Shujing, Li Shanshan. Research Status and Development Trends of Nepenthes Leaf Traps in Engineering Bionics [J]. Journal of Hebei University of Science & Technology, 2018,39(3).

[13] Yan Defeng, Liu Zai, Pan Weihao, et al. Research Status of Manufacturing and Application of Multifunctional Superhydrophobic Surfaces [J]. Surface Technology, 2021,50(5):1-19.

[14] Pan R, Zhong ML. Preparation of superhydrophobic and superhydrophilic surfaces via ultrafast laser and mechanical durability of superhydrophobic surfaces [J]. Science Bulletin, 2019,64(12):1268-1289.

[15] Yang Q, Cheng Y, Fang Z, et al. Femtosecond laser micro/nano fabrication and application of biomimetic super-smooth surfaces [J]. Optoelectronic Engineering, 2025,49(1):210326-1-210326-22.

[16] Guan Xiaoya, Wu Bing, Peng Yi. Research Progress on Superhydrophobic Surfaces in the Field of Anti/Prothrombosis[J]. Journal of Functional Materials/Gongneng Cailiao, 2024,55(1).

[17] Shi Yunyun, Xu Junqi, Su Junhong. Optical, Electrical, and Mechanical Properties of Multicomponent Composite Films and Their Applications [J]. Journal of Applied Optics, 2020,41(2):405-420.